SAE INTERNATIONAL

ARTICLE INFO

Article ID: 03-11-04-0028

doi:10.4271/03-11-04-0028

A Method for Turbocharging Single-Cylinder, Four-Stroke Engines

Michael Buchman, Devarajan Ramanujan, and Amos G. Winter,
Massachusetts Institute of Technology

Abstract

Turbocharging can provide a low cost means for increasing the power output and fuel economy of an internal combustion engine. Currently, turbocharging is common in multi-cylinder engines, but due to the inconsistent nature of intake air flow, it is not commonly used in single-cylinder engines. In this article, we propose a novel method for turbocharging single-cylinder, four-stroke engines. Our method adds an air capacitor-an additional volume in series with the intake manifold, between the turbocharger compressor and the engine intake-to buffer the output from the turbocharger compressor and deliver pressurized air during the intake stroke. We analyzed the theoretical feasibility of air capacitor-based turbocharging for a single-cylinder engine, focusing on fill time, optimal volume, density gain, and thermal effects due to adiabatic compression of the intake air. Our computational model for air flow through the intake manifold predicted an intake air density gain of 37-60% depending on heat transfer rates; this density translates to a proportional to power gain. An experimental setup was constructed to measure peak power, density gain, and manifold pressure. With an air capacitor seven times the volume of engine capacity, our setup was able to produce 29% more power compared to natural aspiration. These results confirm our approach to be a relatively simple means for increasing power density in single-cylinder engines. Therefore, turbocharging single-cylinder engines using an air capacitor can provide a lower cost alternative for increasing the power-output in diesel-powered machinery such as tractors, generators, and water pumps, when compared to adding an additional cylinder.

History

Received: 16 Nov 2017
Revised: 26 May 2018
Accepted: 08 Jun 2018
e-Available: 24 Jul 2018

Keywords

Turbocharging, Manifold, Single-cylinder, Air-capacitor, Diesel

Citation

Buchman, M., Ramanujan, D., and Winter, A., "A Method for Turbocharging Single-Cylinder, Four-Stroke Engines," *SAE Int. J. Engines* 11(4):2018, doi:10.4271/03-11-04-0028.

ISSN: 1946-3936
e-ISSN: 1946-3944

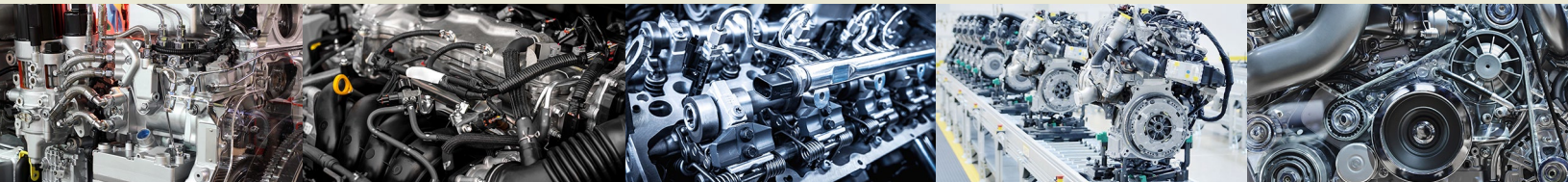

Introduction

A turbocharger in an internal combustion engine consists of a coupled turbine and compressor. The turbine generates rotational energy from the high pressure, high temperature exhaust stream. The compressor uses this energy to increase the density of the intake air. This allows the engine to burn more fuel per cycle, which increases the power output of the engine relative to its naturally aspirated state.

The aim of this research is to turbocharge four-stroke, single-cylinder, internal combustion engines in order to increase their performance relative to naturally aspirated engines. These engines are used in a variety of applications due to their low cost and compact size. They are often selected in devices where minimizing size and weight are critical requirements, such as unmanned aerial vehicles, motorcycles, landscaping equipment, and generators. They are particularly ubiquitous in developing and emerging markets, where they provide a low-cost, high-power solution for water pumping, tractors, and electricity generation.

Benefits of Turbocharging

Advantages of turbocharging include: increased fuel economy, reduced emissions, lower cost per unit power, and reduced weight per unit power [1].

Turbocharging leads to fewer losses and increased fuel economy for two reasons. First, for a desired power level, a turbocharged engine can be sized smaller than a naturally aspirated engine. A smaller engine will produce fewer frictional losses due to less frictional area between the piston and the cylinder. Second, due to larger mass flow rates of air, there is better heat transfer in the engine, which reduces cooling losses [1]. According to Makartchouk [2], turbocharging a diesel engine increases the mechanical efficiency (η) between 2-10%. In practice, most stationary applications for turbocharged engines will result in a 5% efficiency gain compared to a naturally aspirated engine of the same power [2]. It has also been shown that the fuel economy of single-cylinder engines can be improved by increasing intake air density [3]. Turbocharging commercial vehicles can result in a 8-18% increase in fuel economy and a 30% reduction in engine size [4].

Turbochargers increase the power density of engines, which is crucial for weight sensitive applications such as aircraft, and portable equipment such as irrigation pumps on small farms [5, 6]. Increased power density results in a lighter device; this improves fuel economy in commercial vehicles. Studies on turbocharging two-cylinder engines in India showed an increase in power density of 12-13% relative to natural aspiration [7, 8]. In commercial vehicles, turbocharging has been shown to reduce engine size by an average of 30% [4].

Adding a turbocharger to an engine costs between 10-20% of what it would cost to add another cylinder [9]. A study of passenger cars found that there was a $300 advantage in cost of ownership to turbocharging compared to a naturally aspirated engine, despite the added cost of the turbocharger [4].

Turbocharging Single-Cylinder Engines

Multi-cylinder engines are straightforward to turbocharge since the engine cycle can be timed such that when one cylinder is going through the exhaust stroke (powering the turbocharger), another cylinder is intaking [1, 10]. However, in a single cylinder engine, there is a phase difference between the intake and exhaust stroke. This means when the engine is exhausting (and the turbocharger is being powered), the intake valve is closed and the compressed air from the turbocharger has nowhere to flow. Due to the pulsating nature of single cylinder exhaust and the phase mismatch, commercial single cylinder engines are not currently turbocharged, despite the advantages mentioned earlier [11].

A turbocharger attached to a single-cylinder engine will be powered by exhaust pulses that occur once per two crankshaft revolutions. Therefore, the performance of a turbocharged single-cylinder engine is largely determined by the behavior of the turbocharger under pulsating conditions. Studies conducted by Chen and Martinez-Bostas [12] suggest that in this state the turbocharger acts like a pulsating pressure source. Nakonieczny [13] looked at pressure variation in the inlet and exhaust manifolds of a turbocharged engine as a function of crank angle. This study found that pressures in both the inlet and the exhaust manifold fluctuate significantly during the engine cycle, which adds to the evidence that the turbocharger acts as a pulsating pressure source.

This article presents a means for turbocharging single-cylinder engines by buffering intake air between the exhaust and intake strokes using an air capacitor: an additional volume added in series to the intake manifold (Figure 1). The capacitor stores air compressed by the turbocharger during the exhaust stroke, then uses the pressure in the vessel to force air into the cylinder during the intake stroke. It also smoothes the peaky nature of a turbocharger-which behaves like a pulsating pressure source with close to zero inertia [12, 13, 14, 15].

In addition to describing our approach, we analyze the feasibility of adding an air capacitor and a turbocharger to a single-cylinder engine using both theoretical modeling and experimental validation. The goal of the experimental study is to demonstrate real-world applicability of our approach for improving power densities of single-cylinder engines commonly used in the developing world. To this end, we designed our experimental setup around a low-cost, single-cylinder diesel engine and a turbocharger that has been previously used in automobiles in India [16].

Theoretical Modeling

In this section, the theoretical feasibility of the air capacitor is analyzed, focusing on fill time, optimal volume, density

FIGURE 1 Block diagram representation of engine flow with the proposed air capacitor system.

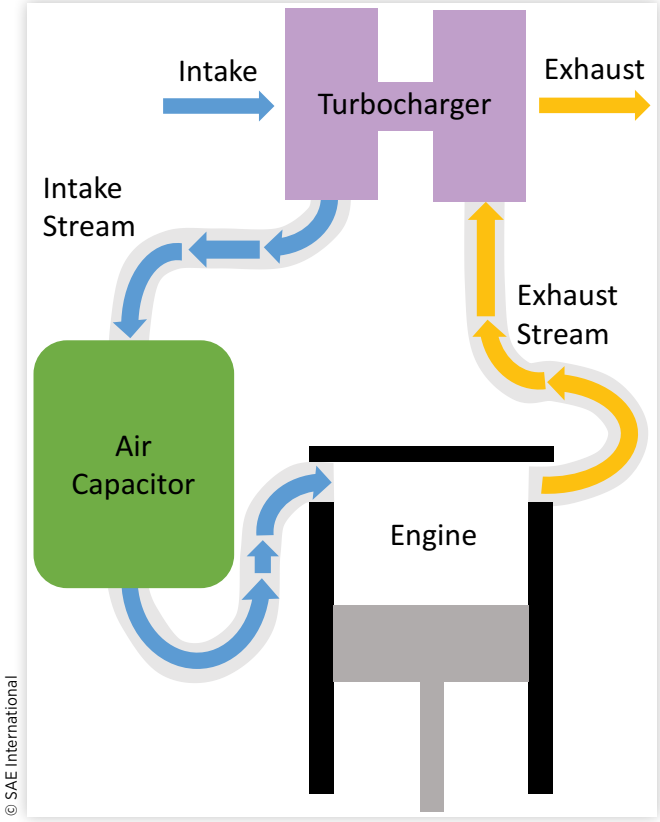

FIGURE 2 Ratio of pressure in the air capacitor to turbocharger operating pressure (P_f/P_t) plotted as a function of the ratio of capacitor volume to engine volume (V_c/V_e). The pressures in this plot are assumed to be measured at the end of an intake stroke. The shaded area represents the optimal capacitor size where significant pressure gain can be achieved before diminishing marginal return.

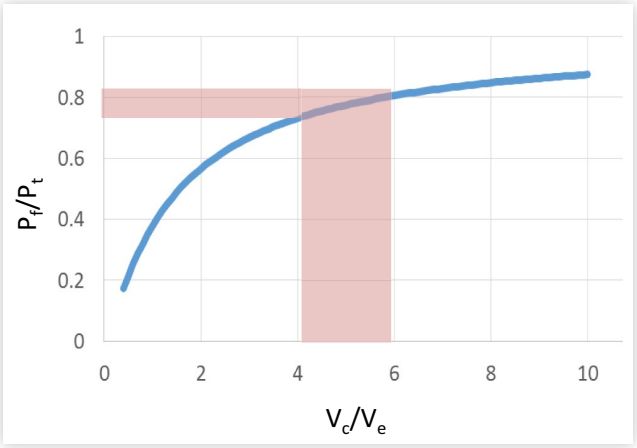

gain that can be achieved by the system, and thermal effects due to adiabatic compression of the intake air. We begin this process by analyzing pressure drop in the manifold during to the intake stroke assuming steady state operation of the engine. Based on these results, a more complex model was built using MATLAB® to include transient effects. Two separate turbocharging models were considered, to predict pressures in the capacitor and the engine. Finally, these models were used to analyze the density of the intake air accounting for thermal and heat transfer effects in the turbocharger.

Single Cycle Capacitor Pressure Drop

The size of an air capacitor is a critical consideration for modeling turbocharger performance. A volume that is too large will cause excess turbo lag due to the pressurization time of the capacitor. A volume that is too small will cause a large drop in the intake manifold pressure during the intake stroke, negating the benefits of the turbocharger [17].

To investigate the effect of capacitor size on air delivered to the engine, we constructed a theoretical model for capacitor pressure drop with the following assumptions: (1) the expansion of air from the capacitor into the cylinder is adiabatic, (2) the pressure inside the capacitor starts at the turbocharger pressure, (3) during the intake stroke, the volume of the system increases to the sum of the volume of the capacitor and the engine, and (4) ideal gas behavior of air.

Equation 1 describes adiabatic expansion of air when treated as an ideal gas in the air capacitor.

$$P_t \cdot V_c^{\gamma} = P_f \cdot (V_e + V_c)^{\gamma}$$

$$\frac{Intake\ \ Pressure}{Turbo\ \ Pressure} = \frac{Pf}{Pt} = \left(\frac{V_c}{V_e + V_c}\right)^{\gamma} \qquad \text{Eq. (1)}$$

The product of pressure (P) and volume raised to the heat capacity ratio (V^{γ}) is constant due to the adiabatic nature of the expansion [18]. The left side of the equation ($P_t \cdot V_c^{\gamma}$) represents the pressure and volume of the capacitor before the intake stroke. The right side ($P_f \cdot (V_e + V_c)^{\gamma}$) represents the state at the end of the intake stroke. The total volume at the end of the intake stroke is equal to the combined volume of the capacitor (V_c) and the engine (V_e). Figure 2 shows the relationship between the pressure delivered by the capacitor divided by the turbocharger operating pressure (P_f/P_t), versus the volume of the capacitor divided by the engine volume (Y_c/V_e). The heat capacity ratio (γ) is taken to be 1.4 [18].

Figure 2 demonstrates that the gain from increasing the volume of the air capacitor diminishes beyond 5 to 6 times the engine volume. Therefore, for a 0.4 L engine-the size tested in this study-gains would significantly diminish for a capacitor 2 to 2.5 L. This is a reasonable size in comparison to other engine components, such as the fuel tank or muffler, which shows adding an air capacitor to an engine is geometrically feasible and could provide performance enhancements.

Multiple Cycle Intake Model

In this section, we describe the theoretical model constructed to characterize air flow from (1) the turbocharger to the capacitor, and (2) the air capacitor to the engine. The goal of constructing the multiple cycle intake model was to analyze the performance of the engine/air capacitor system in transient applications. One of the key factors governing this performance is the time required to pressurize the capacitor to operating pressure and the steady state operating pressure. This is because the time taken for the air capacitor to reach operating pressure will directly contribute to turbocharger lag. To construct the multiple cycle intake model, the following assumptions about the system behavior were made.

- The air capacitor was treated as a varying pressure source.
- The single-cylinder engine was treated as a varying volume of air. The variation in volume is driven by the opening and closing of the intake valve that in turn depends on the phase angle of the crankshaft.
- Two different models for the turbocharger were considered: the infinite inertia model (IIM), and the zero inertia model (ZIM). Details on these two models are provided below.

The IIM treats the turbocharger as a constant pressure source, as presented in the previous section. The basic premise in this model is that the turbocharger-rotor has infinite inertia and therefore never slows down. This results in no variation in turbocharger pressure. On the other hand, the ZIM treats the turbocharger as an intermittent pressure source that only turns on when the engine is powering it during the exhaust stroke.

The ZIM assumes that the turbocharger instantaneously spools up and comes to a halt at the end of the exhaust stroke. While these models provide theoretical bounds for turbocharger performance, a turbocharger's real-world behavior will lie in between these two models. Previous work predicts that it will probably lie closer to the ZIM [12].

The theoretical model was constructed to characterize the pressure in the air capacitor as a function of turbocharger pressure. Here we used the IIM/ZIM to characterize turbocharger behavior. This analysis gave the bounds on the real-world performance of the turbocharger. The flow along the streamline that runs from the pressure source to the center of the air capacitor (streamline 1 in Figure 3) was calculated using conservation of mass, the ideal gas law, and the Bernoulli equation [15]. For this streamline, the velocity of air was approximated as zero inside the capacitor. Additionally, in Equations 2-8 air flow was assumed to be steady and incompressible [1, 13, 18]. The streamline from the center of the air capacitor to the engine cylinder (streamline 2 in Figure 3) was also described by a differential equation derived in a similar manner as the first streamline [15]. Both models (IIM/ZIM) had the same governing equations for air flow (Equations 2-8). The difference between the two models was a result of different boundary conditions applied to the inlet pressure as a function of time.

FIGURE 3 Block diagram depiction of the flow in the ZIM and IIM models.

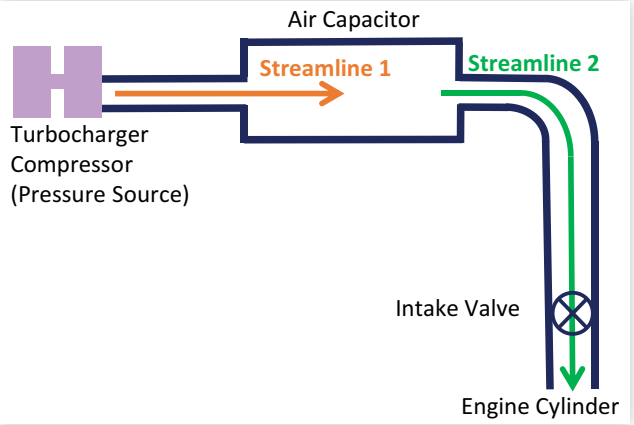

The flow along streamline 1 shown in Figure 4 can be described by the modified Bernoulli equation, which also accounts for pipe losses [18].

$$\frac{P_t - P_c}{\rho_t} = \left(1 + \frac{FL}{2D} + \frac{k}{2}\right) v_s^2 \qquad \text{Eq. (2)}$$

Mass flow from the pressure source as a function of density, velocity, and the cross-sectional area of the connecting tube is defined as [18]

$$\dot{m}_s = \rho_t v_s A. \qquad \text{Eq. (3)}$$

The ideal gas law can then be used to calculate the mass flow into the air capacitor [18].

$$\dot{m}_c = \frac{\dot{P}_c V_c}{R T_c} \qquad \text{Eq. (4)}$$

Due to mass conservation, the mass flow rate out of the constant pressure source will be equal to the mass flow rate into the air capacitor [18].

$$\dot{m}_c = \dot{m}_s \qquad \text{Eq. (5)}$$

The velocity of the air in the connecting tube can be calculated by combining Equations 3-5.

$$\rho_t v_s A = \frac{\dot{P}_c V_c}{R T_c}$$
$$v_s = \frac{\dot{P}_c V_c}{\rho_t A R T_c} \qquad \text{Eq. (6)}$$

To solve for the pressure in the capacitor, Equations 1 and 6 are combined to eliminate the velocity term.

$$\frac{P_t - P_c}{\rho_t} = \left(1 + \frac{FL}{2D} + \frac{k}{2}\right) \frac{\dot{P}_c^2 V_c^2}{\rho_t^2 A^2 R^2 T_c^2}$$
$$P_t - P_c = \left(1 + \frac{FL}{2D} + \frac{k}{2}\right) \frac{\dot{P}_c^2 V_c^2}{\rho_t A^2 R^2 T_c^2} \qquad \text{Eq. (7)}$$

A parameter C that includes the friction factor and velocity is derived in Equation 8. Variations in the friction

FIGURE 4 (A) Engine and capacitor pressure profiles plotted using the IIM for the turbocharger. (B) Single engine cycle for the IIM. Engine pressure is only shown for the intake stroke since the model only looks at the engine during the intake stroke. This model assumes the air capacitor starts at atmospheric pressure and temperature, a 0.9 bar turbo pressure, air capacitor volume as 5 times engine volume, and an engine speed equal to 3600 RPM.

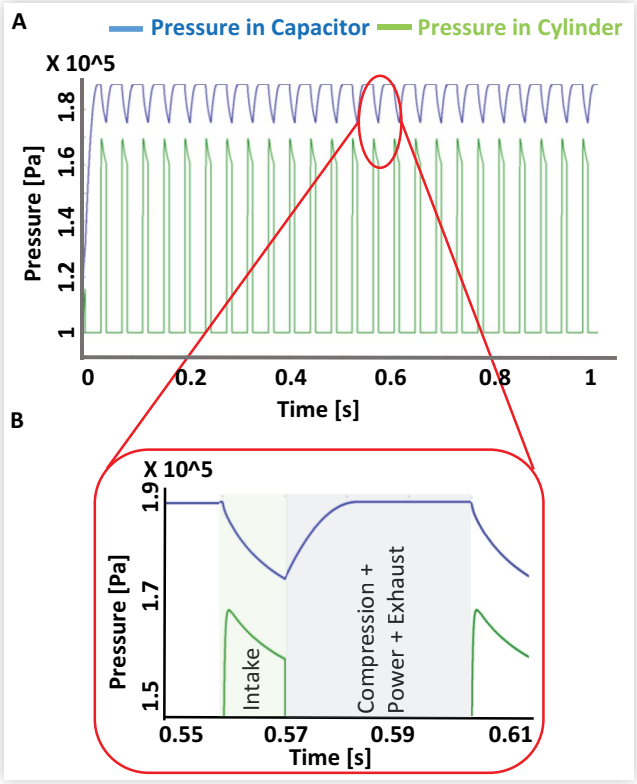

factor are assumed to be small enough that C can be treated as a constant. A nonlinear first order differential equation that describes the pressure inside the capacitor as a function of the turbo pressure is derived (see Equation 9). This allows us to solve for C iteratively based on small changes in pressure. Since Equation 9 is solved by breaking the problem into small time steps, the friction factor approximation does not result in a noticeable error.

$$C = \frac{\rho_t A^2 R^2 T_c^2}{\left(1 + \frac{FL}{2D} + \frac{k}{2}\right) V_c^2} \qquad \text{Eq. (8)}$$

$$P_t - P_c = \frac{1}{c}\dot{P}_c^2$$

$$\dot{P}_c^2 + C \cdot P_t - C \cdot P_c = 0 \qquad \text{Eq. (9)}$$

The ZIM uses the boundary condition that P_t is equal to the turbo pressure during the exhaust stroke and that during the other three strokes there is no flow between the capacitor and the turbocharger. The IIM model uses the boundary condition that P_t is always equal to the turbo pressure.

Our analysis is conducted for a characteristic engine using the following parameters: a 2.0 L capacitor, 0.9 bar turbo pressure, a 0.418 L engine, 3000 RPM engine speed, and a compression ratio of 18:1. These steady state parameters were based on the diesel engine that was chosen for our experimental setup.

Figure 4 illustrates the transient response of the air capacitor using the IIM. The capacitor reaches steady state in approximately 0.15 s with a pressure nearly equal to the turbocharger's pressure (0.9 bar). Figure 4 also shows the response of the system during one engine cycle (note that the engine's pressure is only plotted during the intake stroke). During the intake stroke, the pressure in the capacitor drops until it is equal to the engine pressure minus the pressure drop due to flow losses. Then pressures in the engine and the capacitor decrease together for the remainder of the intake stroke. During the compression, power, and exhaust strokes, pressure in the capacitor increases rapidly. A limitation of this model is that it does not capture the spool-up time required for the turbocharger, which will result in a significant underestimation of startup time.

Figure 5 shows the transient pressure response for the air capacitor, using the ZIM for the turbocharger (engine pressure is only plotted during the intake stroke). The capacitor reaches steady state in approximately 0.5 s and provides an intake cylinder pressure of approximately 50% over atmospheric pressure. Figure 5 also shows the pressure response in the engine and capacitor over a single engine cycle. During the intake stroke, the pressure in the capacitor drops until it becomes close to the engine pressure and then drops further as the piston moves downward and the cylinder fills with air. The difference between the intake and capacitor pressure can be explained by pipe losses. The capacitor pressure remains constant during the compression and power stroke and then increases rapidly during the exhaust stroke.

Multiple Cycle Thermal Intake Model

To get a more accurate model of density gain in the capacitor, thermal effects were taken into account. In the air capacitor, adiabatic compression by the turbocharger results in a pressure gain proportionally larger than the density gain in the intake air. This effect of adiabatic compression on the temperature of an ideal gas is described in a form of the ideal gas law (Equation 10) [18]. Temperature's effect on density is defined as [18].

$$T_c = T_0 \left(\frac{P_c}{P_0}\right)^{\left(\frac{\gamma-1}{\gamma}\right)} \qquad \text{Eq. (10)}$$

$$\rho_c = \frac{P_c}{R T_c} \qquad \text{Eq. (11)}$$

FIGURE 5 (A) Engine and capacitor pressure profile using the ZIM for the turbocharger. (B) Single engine cycle for the ZIM. Engine pressure is only shown for the intake stroke since the model only looks at the engine during the intake stroke. This model assumes the air capacitor starts at atmospheric pressure and temperature, a 0.9 bar turbo pressure, air capacitor volume as 5 times engine volume, and an engine speed equal to 3600 RPM.

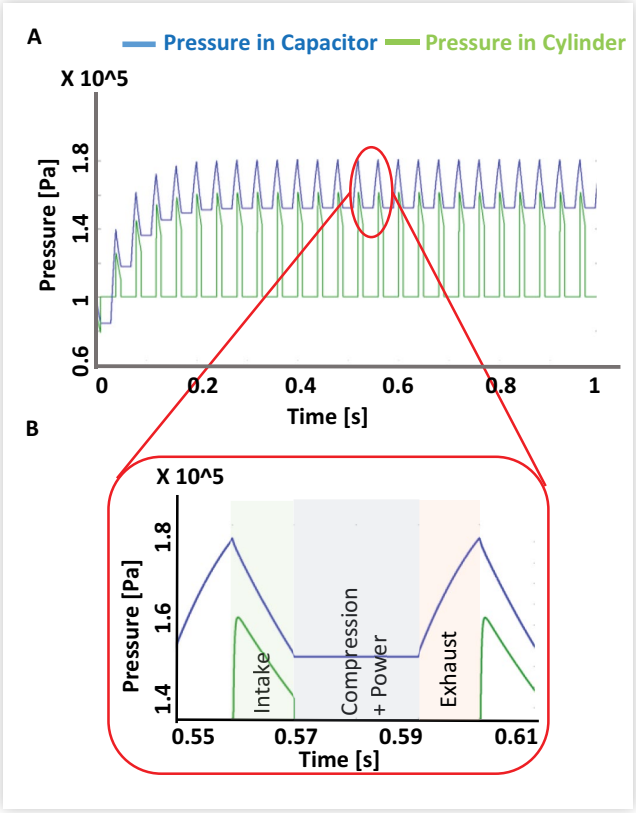

Density changes as a function of pressure change in adiabatic conditions can be solved by combining Equations 10 and 11 into Equation 12.

$$\frac{\rho_c}{\rho_0} = \left(\frac{P_c}{P_0}\right)^{\left(\frac{1}{\gamma}\right)} \qquad \text{Eq. (12)}$$

The ZIM for the turbocharger was expanded using Equation 11 to account for density gain in the air capacitor with and without cooling. The ZIM was chosen over the IIM to characterize the system because it represents a more conservative estimate of modeling turbocharger behavior, and literature suggests that it is closer to how a turbocharger under pulsating inlet conditions will behave [19].

The results of this model are shown in Figure 6. Here, the same operating parameters from the previous section were used. Figure 6 describes density variation in the air capacitor under the ZIM model for two specific cases: (1) assuming no heat transfer between the capacitor and the environment, and

FIGURE 6 Plots showing density decrease in the capacitor due to thermal effects of adiabatic compression. (A) Steady state density variation as a function of capacitor size in the using the ZIM model. The analysis is done for a non-dimensional capacitor size that is normalized to the engine volume V_C/V_E. (B) The effect of heat transfer on the transient response for an air capacitor with $V_C = 5V_E$ (represented by the red points in Figure 6A). This model assumes 0.9 bar turbo pressure and a 3600 RPM engine speed.

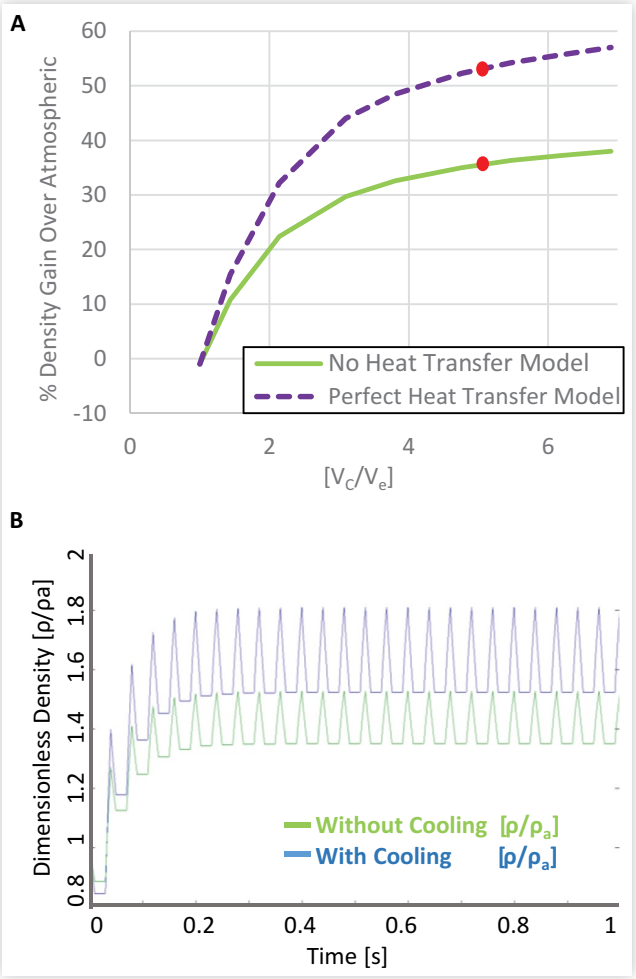

(2) assuming perfect heat transfer. In the no heat transfer case, intake air density was found to be approximately 35% higher than atmospheric density. To a first order approximation (assuming volume of fuel that can be burned is proportional to the volume of air in the cylinder), this increase in density would correspond to a 35% increase in engine power, compared to natural aspiration. Adding an intercooler to the intake system would increase intake air density even more, consequently increasing engine power. Perfect cooling of the air to ambient temperature would, to a first order approximation, increase engine power by approximately 55%, compared to natural aspiration. In reality, the system should operate somewhere between these two extreme cases.

Experimental Setup

The primary goal of the experiment was to demonstrate that an air capacitor-based turbocharging system can improve the power density of a single-cylinder engine, and to demonstrate how engine performance varies with different size air capacitors. An important consideration in this experiment is the use case context for this technology: off-grid power applications in the developing world. Therefore, the cost of our setup, as well as its applicability to developing world markets, were significant decision factors when designing the experiment.

Six dependent variables were measured to characterize the performance of the air capacitor based turbocharging system: (1) intake air density, (2) engine speed, (3) intake pressure, (4) exhaust pressure, (5) compressor pressure, and (6) intake temperature. The two independent variables chosen for the study were capacitor size and power output. Our aim was to verify the viability of the air capacitor using these metrics.

Setup Description

The experimental setup consisted of a dynamometer built around a four-stroke, single-cylinder diesel generator (Figure 7). The engine selected for the experimental setup was a Koop model KD186FA. This engine was chosen based on the following decision criteria: a relatively large capacity (0.418 L), an 18:1 compression ratio [20, 21], applicability to developing world contexts (low cost, made in China), and the generator form factor (makes it easy to build a dynamometer around). The engine was rated for 10 horsepower and the generator unit was rated for a peak power output of 6500 W [22]. The engine is designed to run continuously at 3600-3700 RPM to produce a 120 V 60 Hz AC power output load [22].

For turbocharging this engine, a Garrett GT0632SZ turbocharger was fitted to the setup. It is one of the smallest turbochargers available and is designed for engines between 0.1 and 0.5 L. It has a peak turbo pressure of 0.9 bar [23] and is used by Tata Motors (an Indian automobile manufacturer) on some of their two-cylinder products [16]. A separate oil system was fitted to the turbocharger for lubricating the bearings. For the given operating case-0.9 bar inlet pressure, engine intake density of 1.7 kg/m^2, 0.42 L engine with a speed of 3700 rpm, and a corrected air flow of ~2.9 lbs/min-the turbocharger's compressor is approximately 64% efficient and operates at 230,000 RPM (determined from the manufacturer issued turbocharger map) [24].

The intake manifold was modified with an adapter that converted the stock engine intake fitting into a female, one-inch NPT pipe fitting, which allowed different sized air capacitors to be attached to the engine. The adapter was fitted with a temperature sensor and a pressure sensor, placed in close proximity to the engine to obtain intake air density. Six capacitors were made with sizes ranging from 0.4 to 2 L (total intake manifold volume of 1.3-2.9 L when including the volume of the piping). The system was also tested without a capacitor (total intake manifold volume of 0.9 L).

FIGURE 7 Picture of the dynamometer used in the experimental setup. The top pane shows an overview of the system. The middle pane shows the operator control panel. The bottom pane shows a detailed view of the custom intake and exhaust manifolds.

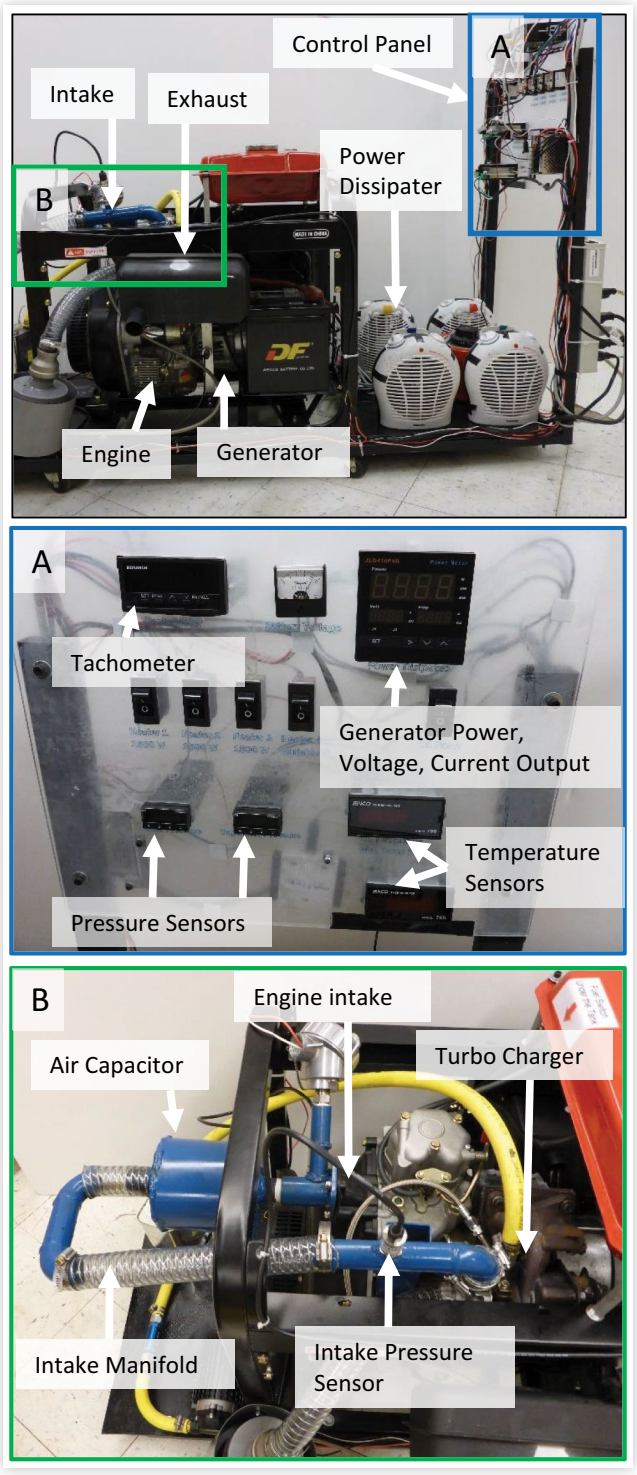

Six space heaters were used to provide a controlled load on the engine. Each heater could deliver a load of up to 1500 W. Three of the space heaters were wired to the generator through operator-controlled switches, and two were plugged directly into the generator. The sixth space heater was wired to the generator through a variable AC power transformer, allowing it to generate a load between 0-1500 W. As a result, the power dissipation system could provide a load in the range of 0-9000 W on the engine. The load on the engine was measured by a power meter that displayed the voltage, current, and dissipated power from the generator. An optical tachometer was installed to measure engine speed. We also installed pressure sensors that monitored: compressor pressure, intake pressure, and the exhaust pressure. Finally, to calculate air density, intake temperature was measured. The measurements were taken by an operator reading the gauges.

Experiments Conducted

For each capacitor size (0.9, 1.3, 1.6, 2, 2.3, 2.6, and 2.9 L), three experiments were run: (1) the cold peak power test measured the peak power of the engine after cold start; (2) the manifold characterization test measured manifold pressures, power output, and intake temperature; and (3) the hot peak power test measured sustained peak power by slowly increasing the load on the engine and logging engine characteristics at different loads until manifold pressures started to vary significantly. From this point on, the load was increased until the engine stalled. This allowed us to measure hot peak power.

Due to the time involved to run trials and reset the experimental setup (a day per experiment), one test was done for each sized capacitor. For each capacitor, intake pressure, compressor pressure, exhaust pressure, and intake temperature were measured at 750 W power dissipation increments (determined based on the wattage of the space heaters used to load the engine). Error ranges for peak power were determined by calculating the aggregate sensor error. For manifold pressure and density tests, the engine was run in steady state and data was logged for approximately 5 min. For these tests the error bars represent the maximum and minimum values measured.

Results and Discussion

Density Gain Results

Density gain is defined as the percent increase of the intake density over the ambient air density and is calculated from intake temperature and pressure using the ideal gas law. Our experimental setup was able to measure intake air density obtained for all capacitors up to about 70% of peak power. Beyond this, the pressure in the capacitor fluctuated too significantly to get accurate readings. Figure 8 shows the maximum measured density gain for the seven different sized capacitors. The number next to each point is the load on the generator at which the maximum density gain measurement was taken.

FIGURE 8 Measured maximum density gain compared to the temperature adjusted ZIM. The number next to each point represents the power at which peak density gain was measured. This power is less than the peak power output due to large pressure fluctuations at higher loads. The error bars represent the maximum and minimum measured density gain at each point. The two lines represent the predicted density gain with and without heat transfer in the capacitor.

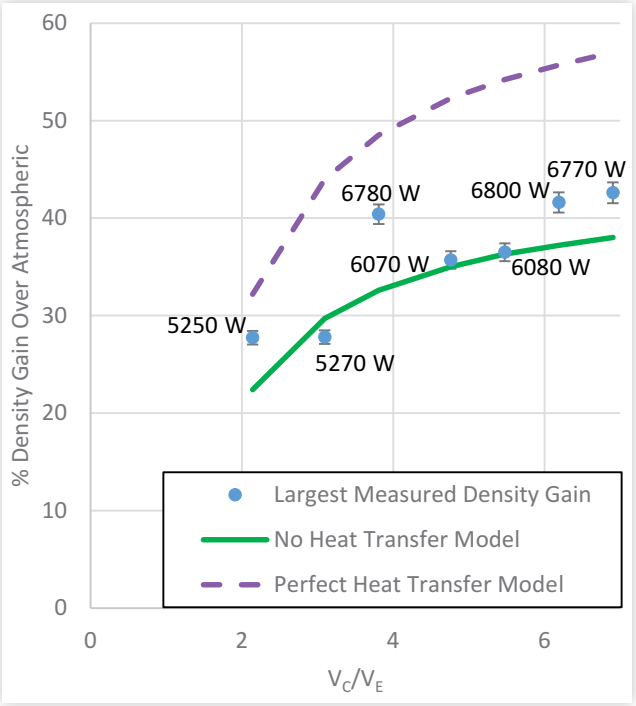

The measurements were taken at the maximum power where the pressure in the capacitor fluctuated less than 0.07 bar. As a result, the measured peak density is most likely less than the actual peak density (defined as density at peak power). This also means that the points on the plot were taken at different power levels and, therefore, do not represent a trend of how density varies with capacitor sizes.

Figure 9 illustrates the relationship between intake density gain and load on the generator. This relationship is close to linear; as the load on the generator increases, the intake density also increases. This demonstrates that the system is behaving as expected. As seen in Figure 9, the naturally aspirated density gain is negative due to flow losses over the air filter and heat addition from the engine.

Peak Power Results

Cold and hot peak power were measured for the seven air capacitor sizes and the naturally aspirated case (Figure 10). With the largest sized capacitor (2.9 L), peak power increases of up to 29% and 18% were observed for the cold and hot power

FIGURE 9 Variation of percent density gain of the intake air plotted as a function of power dissipated. Plot shows the naturally aspirated case and the turbocharged cases for the largest and smallest capacitor.

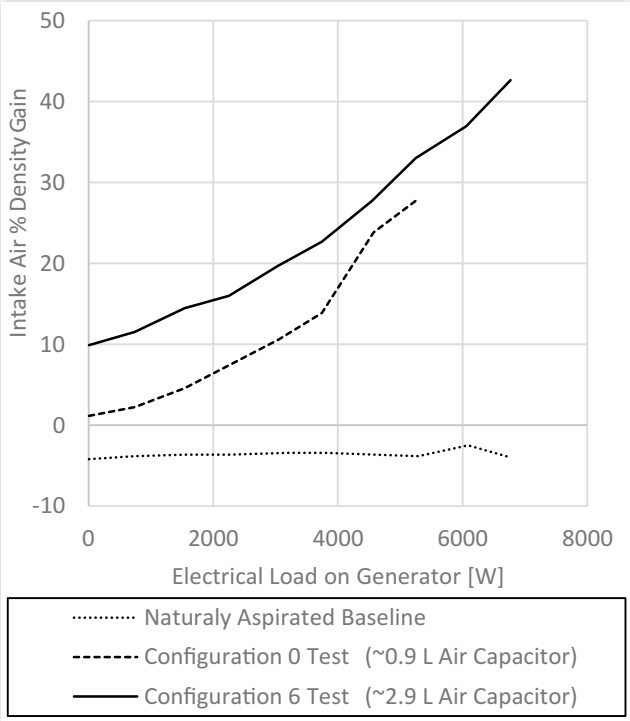

FIGURE 10 Measured peak power values compared to temperature adjusted, zero inertia model (ZIM). The error bars represent instrument error which is the rated sensor error.

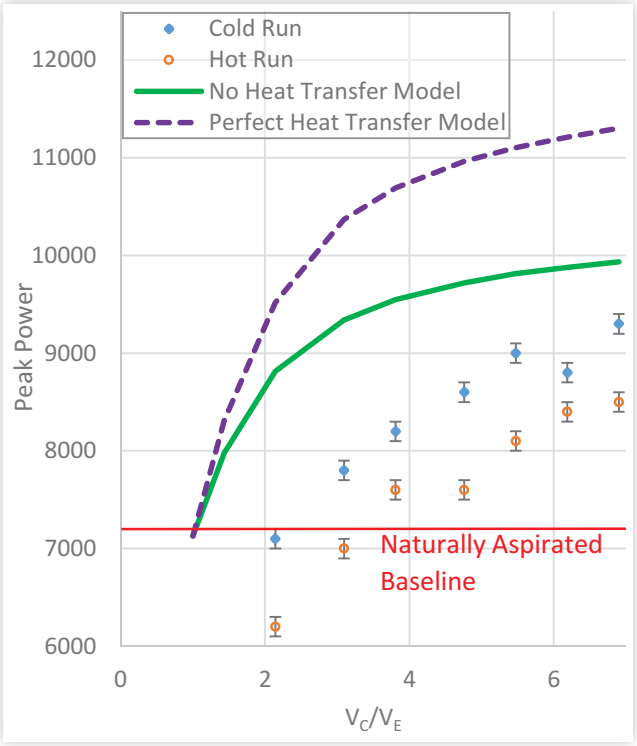

case, respectively. Cold peak power is important for the intermittent use case while the hot peak power is important for the steady state use case, as cold peak power is the power output available for short intervals.

We observed the system to have the same trend as predicted by the ZIM with the no heat transfer model. As expected, increasing capacitor size increased peak power. However, the observed peak power was significantly less than the values predicted by the model. This could be due to a combination of factors such as ambient conditions, engine intake leakage, exhaust gas drifting back into the engine, and elevated exhaust pressure. Despite these factors (which negatively affect the engine's power output), the experimental setup was able to generate significantly more peak power (+29% cold peak power gain) when compared to the naturally aspirated case.

The maximum measured density gain was about 45% greater than the naturally aspirated engine's density. However, the adjusted peak power of the engine (Figure 11) was only 29% greater. This suggests density and power gain are not matching as predicted by the ZIM with no heat transfer. This is due to errors (discussed in the error analysis).

Manifold Pressure Results

This section focuses on characterizing intake and exhaust pressures in the engine manifold. For this, data were obtained from three pressure sensors placed: (1) after the capacitor at the engine's intake, (2) right after the compressor, and (3) in the exhaust manifold. These pressures were used to determine turbocharger behavior, the effect of back pressure on the system, and compressor pressure.

Figure 11 shows the gauge pressure in the capacitor as a function of load on the generator. This view of the data is useful for understanding how pressure varies with load and comparing the turbocharged data with the naturally aspirated baseline. From Figure 11, it is clear that as load on the generator increases so does the intake pressure. Note that the naturally aspirated intake pressure is negative due to flow losses across the air filter as well as heat addition from the engine. The measured peak pressure was 0.66 bar, which was 74% of the turbocharger's waste-gate pressure (0.9 bar). This number is also less than the actual peak pressure in the cylinder, as pressure was measured up to a generator load of 6800 W, while the turbocharged engine was able to produce 9300 W of output power.

We also examined the correlation between exhaust pressure differential with generator load and capacitor size. An increase in exhaust pressure differential is detrimental as it decreases peak power. This occurs due to an increase in pumping losses and incomplete scavenging after the exhaust stroke. Figure 12 illustrates the variation in exhaust pressure differential with respect to the load on the generator and the naturally aspirated baseline. As seen for the turbocharged

FIGURE 11 Variation of intake pressure as a function of power dissipated. Plot shows the naturally aspirated case and the turbocharged case for the largest and smallest capacitor.

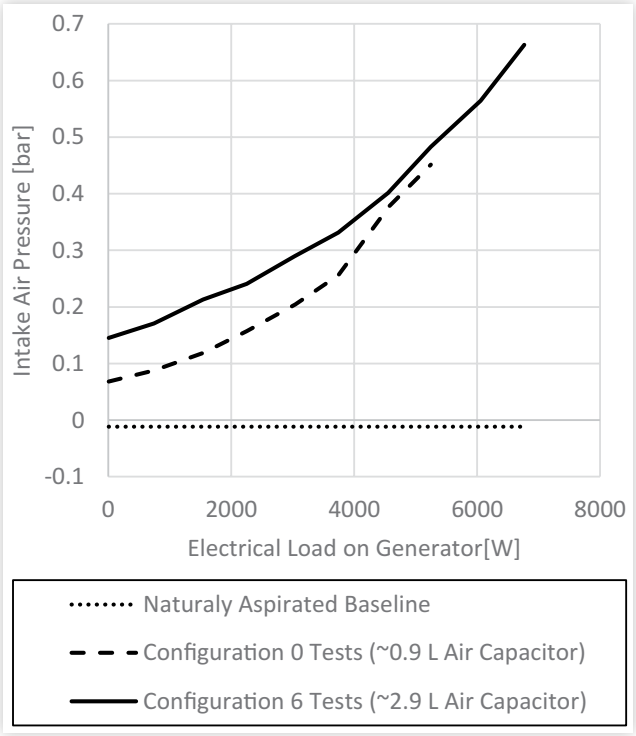

FIGURE 12 Exhaust pressure differential (difference in pressure between the exhaust and intake manifolds) as a function of power dissipated. Plot shows the naturally aspirated case and the turbocharged case for the largest and smallest capacitor.

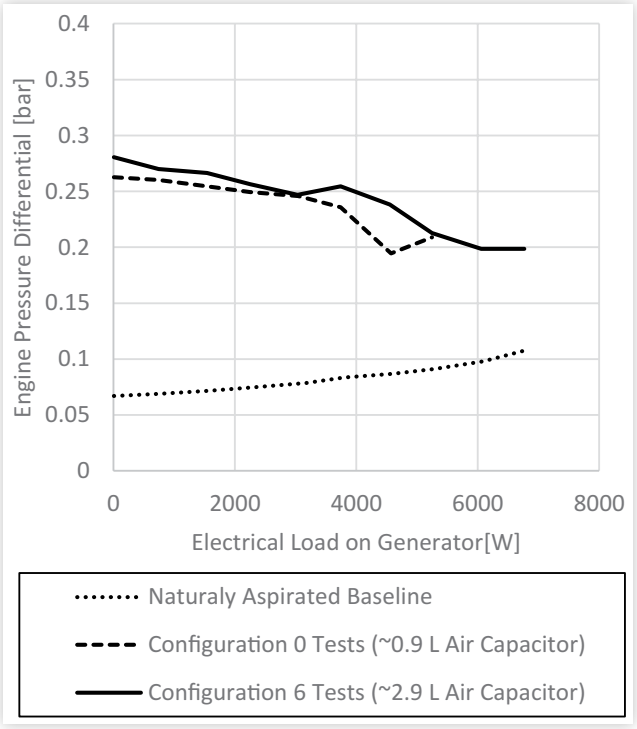

case, an increase in generator load decreases exhaust pressure. This relationship is inverted for the naturally aspirated baseline, wherein exhaust pressure differential increases with generator load. For the turbocharged case, the exhaust pressure differential most likely decreases with increased generator load due to higher enthalpy exhaust gas increasing the intake pressure. For the naturally aspirated case, the exhaust pressure differential increases with generator load probably because the increase in exhaust temperature at higher engine loads increases exhaust pressure. For all cases, the exhaust pressure differential is noticeably larger in the turbocharged case than it is in the naturally aspirated case. The difference ranges from approximately 0.2 bar, when there is no load on the generator, to about 0.1 bar at 6.8 kW of load on the generator. This increase is probably due to the added flow resistance of the turbine, the new exhaust manifold, and the muffler connector. The increase in exhaust pressure partially accounts for the mismatch in the peak power and density gains predicted by the ZIM with no heat transfer when compared to experimental results.

Sources of Error

Results from the experiments confirm the feasibility of our approach to add a turbocharger to a four-stroke, single-cylinder engine using a large volume intake manifold. Results also show that capacitor size has a significant effect on the performance of the single-cylinder engine. Overall, the experiment was successful in validating that: (1) air capacitor-based turbocharging of single-cylinder engines is feasible and can improve the power density of a single-cylinder engine; (2) intake manifold properties significantly affect the engine operating characteristics; and (3) trends for power output as a function of capacitor size can predicted by the ZIM model.

We observed a deviation of 9-30% between the experiment and the model due to discussed experimental errors. There were a few possible sources of error that could have contributed to this mismatch. The first possible source of error was that the theoretical model did not take exhaust pressure differential into account. An elevated exhaust pressure differential causes an increase in pumping losses and, as a result, a decrease in peak power. Additionally, it would lead to more exhaust mass left in the cylinder after the exhaust stroke, which would also decrease power. A second possible source of error was air leakage in the intake manifold. Since this engine was designed to be naturally aspirated, the intake manifold was not leak-proofed for operating under positive pressure. This led to significant leakage which was observed by the operator. This leakage would have resulted in a density reduction of the air flowing into the engine cylinder, which would cause a reduction in peak

power. The third potential source of error was exhaust gas getting pulled into the intake. While the tests were conducted outside, the area they were conducted in had poor air circulation. Therefore, exhaust gas could have been pulled into the intake stream causing less oxygen to enter the engine and a net decrease in peak power. The operator noticed this effect at higher power levels as he spotted dark-colored exhaust gas near the intake.

Conclusions and Future Work

This article presents a novel method for turbocharging four-stroke, single-cylinder internal combustion engines. We analyzed the theoretical feasibility of air capacitor-based turbocharging of a single-cylinder engine.

Two approaches for modeling the turbocharger-the zero inertia, and the infinite inertia model-were investigated. We found that the ideal air capacitor size was 5-6 times the engine volume. This size was used in flow models which accounted for density variation in the intake air stream under two specific conditions: no heat transfer, and perfect heat transfer. Our results predicted an intake air density gain of 37-60% and transient response time under 1 s. This increase in intake air density results in an increase in power output from the engine, making a case for air capacitor-based turbo charging of single-cylinder engines.

An experimental setup was constructed to validate the feasibility of our approach and compare peak power and density gains with those predicted by the theoretical model. With an air capacitor seven times the volume of engine capacity, our setup was able to produce 29% more power compared to natural aspiration. These results confirm our approach to be a relatively simple means for increasing power density in single-cylinder engines. From a cost perspective, it is estimated that adding a turbocharger adds approximately 20% of the cost of adding a second cylinder (doubling the power) [9]. This implies, at the very least, turbocharging adds 50% more power per unit cost.

The overarching goal of this work was to create a technology that can become commercially viable in developing word contexts. Subsequent work will focus on creating a general method for optimizing a single-cylinder, turbocharged engine around three key factors: peak power, fuel economy, and emissions. To achieve this, our future research will focus on addressing the limitations identified in the theoretical models and the current experimental setup. Specifically, the current computational model will be refined to better predict the peak power output from turbocharging. New models will also be created in order to predict emissions impact and fuel economy. Based on these models, a more complex experiment will be devised that will allow for measurement of fuel economy and emissions impact. As this work has established the feasibility of our approach, our future work will also focus on variables such as emissions quality, capacitor geometry, and fuel efficiency, which are critical for the commercial success of the overall project.

Contact Information

Amos G. Winter
awinter@mit.edu

Michael Buchman
Mbuchman@mit.edu

Acknowledgements

We would like to thank Ari Frankel, Kevin Cedrone, and the members of the Global Engineering and Research Lab (especially Dan Dorsh) for their assistance and feedback on this project. This work was sponsored by the Tata Center for Technology and Design at MIT and the MIT Department of Mechanical Engineering.

This material is based upon work supported by the National Science Foundation Graduate Research Fellowship under Grant No. 1122374. Any opinion, findings, and conclusions or recommendations expressed in this material are those of the authors(s) and do not necessarily reflect the views of the National Science Foundation.

Definitions/Abbreviations

A - Cross sectional area of connecting tube
D - Diameter of connecting tube
F - Friction factor
K - Minor losses
L - Length of connecting tube
$\mathbf{m_c}$ - Mass of gas inside capacitor
$\dot{\mathbf{m}}_\mathbf{c}$ - Mass flow rate of gas into capacitor
$\dot{\mathbf{m}}_\mathbf{s}$ - Mass flow rate of gas out of pressure source
$\mathbf{P_c}$ - Pressure inside capacitor
$\mathbf{P_f}$ - Final Pressure (at the end of intake stroke)
$\mathbf{P_t}$ - Turbocharger pressure
$\mathbf{P_0}$ - Initial pressure inside capacitor
$\dot{\mathbf{p}}_\mathbf{c}$ - Rate of pressure change inside the capacitor
R - Specific gas constant
$\mathbf{T_c}$ - Temperature inside the capacitor
$\mathbf{T_0}$ - Ambient temperature
$\mathbf{V_c}$ - Capacitor volume
$\mathbf{V_e}$ - Engine volume
$\mathbf{v_s}$ - Velocity of air in connecting tube
$\boldsymbol{\gamma}$ - Heat capacity ratio (1.4 for air)
$\boldsymbol{\rho_c}$ - Density of air inside capacitor
$\boldsymbol{\rho_t}$ - Density of air at the turbocharger
$\boldsymbol{\rho_0}$ - Atmospheric density of air

References

1. Watson, N. and Janota, M., *Turbocharging the Internal Combustion Engine* (New York, NY: John Wiley & Sons, 1982).
2. Makartchouk, A., *Diesel Engine Engineering: Thermodynamics, Dynamics, Design, and Control* (New York, NY: Marcel Dekker, Inc, 2002).
3. Tanin, K.V., Wickman, D.D., Montgomery, D.T., Das, S., and Reitz, R.D., "The Influence of Boost Pressure on Emissions and Fuel Consumption of a Heavy-Duty Single-Cylinder D.I. Diesel Engine," SAE Technical Paper 1999-01-0840, 1999, doi:10.4271/1999-01-0840.
4. Dominique Petitjean, C.M., Bernardini, L., and Shahed, S.M., "Advanced Gasoline Engine Turbocharging Technology for Fuel Economy Improvements," SAE Technical Paper 2004-01-0988, 2004, doi:10.4271/2004-01-0988.
5. Pawar, S., "Farm Mechanization in India," presented to the Indian Parliament by the Indian Dept. of Agriculture and Cooperation Mechanization and Technology Division, 2013.
6. Mehta, C.R., "Agriculture Mechanization Strategies in India," presented to Central Institute of Agricultural Engineering, Bhopal Indian Council of Agricultural Research, New Delhi, India, 2013.
7. Bhat, P.G., Thipse, S., Marathe, N.V., Pawar, N. et al., "Upgradation of Two Cylinder NA Diesel Genset Engine into TCIC configuration for Achieving Stricter Emission Norms for 19 kW to 75 kW Power Categories," SAE Technical Paper 2015-26-0097, 2015, doi:10.4271/2015-26-0097.
8. Honeywell Turbo Technologies, Corporate, 2015, http://turbo.honeywell.com/our-technologies/small-wastegate-turbo/.
9. Aravand, B. and Simhachalam, J., Conversion with partners at Mahindra and Mahindra Corporation, 2013.
10. Hiereth, H. and Prenninger, P., *Charging the Internal Combustion Engine* (Vienna: Springer, 2003).
11. Bisane, R. and Katpatal, D., "Experimental Investigation and Analysis of an Single-Cylinder Four Stroke Twin Charged C.I Engine," *Int. J. Res. Eng. Technol.* 205-210, 2014.
12. Chen H., Hekeem, I., and Martinez-Botas, R.F., "Modelling of a Turbocharger Turbine Under Pulsating Inlet Conditions," *Proc. Inst. Mech. Eng. Part J. Power Energy* 210(5):397-408, 1996.
13. Nakonieczny, K., "Entropy Generation in a Diesel Engine Turbocharging System," *Nadbystrzycka* 36(20):1027-10560, 2001.
14. Winter, A.G., "Turbocharged Single-Cylinder Internal Combustion Engine Using an Air Capacitor," U.S. Patent 20150007560A1, 2015.
15. Buchman, M. and Winter, A., "Method for Turbocharging Single-Cylinder Four Stroke Engine," *ASME IDETC & CIE*, Buffalo, NY, 2014.
16. TurboMaster, "Turbocharger Applications," 2015, http://www.turbomaster.info/.
17. Winterbone, D. and Pearson, R., *Design Techniques for Engine Manifolds* (United Kingdom: Professional Engineering Pub. Limited, 1999).
18. Lermusiaux, P., 2.006 Equation Sheet (MIT, 2012).
19. Chan, S., "Thermodynamics in a Turbocharged Direct Injection Diesel Engine," *Proc. Inst. Mech. Eng. Part J. Automob. Eng.* 212:10-24, 1998.
20. Co, Y., *Yanmar Service Manual* (Yanmar, 2015).
21. Wuix Pipor Power Corporation, Kipor Power Operation Manual Version 1 (Kipur, 2010).
22. Depot, H., "6,500-Watt 10 HP Diesel Generator with Electric Start Battery," 2015, http://www.homedepot.com/.
23. Turbomaster, "Garrett GT1241," Retail, 2015, http://www.turbosbytm.com/gt1241.
24. Garrett, "Turbocharger Products," 2015, http://www.turbobygarrett.com/turbobygarrett/.